

The TPLATE Adaptor Complex Drives Clathrin-Mediated Endocytosis in Plants

Astrid Gadeyne,^{1,2,12} Clara Sánchez-Rodríguez,^{3,12} Steffen Vanneste,^{1,2} Simone Di Rubbo,^{1,2} Henrik Zauber,³ Kevin Vanneste,^{1,2} Jelle Van Leene,^{1,2} Nancy De Winne,^{1,2} Dominique Eeckhout,^{1,2} Geert Persiau,^{1,2} Eveline Van De Slijke,^{1,2} Bernard Cannoot,^{1,2} Leen Vercruysse,^{1,2} Jonathan R. Mayers,⁴ Maciek Adamowski,^{1,2,5} Urszula Kania,^{1,2,5} Matthias Ehrlich,³ Alois Schweighofer,^{3,6} Tijs Ketelaar,⁷ Steven Maere,^{1,2} Sebastian Y. Bednarek,⁴ Jiří Friml,^{1,2,5} Kris Gevaert,^{8,9} Erwin Witters,^{10,11} Eugenia Russinova,^{1,2} Staffan Persson,^{3,13,*} Geert De Jaeger,^{1,2,13} and Daniël Van Damme^{1,2,13,*}

¹Department of Plant Systems Biology, VIB, Technologiepark 927, 9052 Gent, Belgium

²Department of Plant Biotechnology and Bioinformatics, Ghent University, 9052 Gent, Belgium

³Max-Planck-Institut für Molekulare Pflanzenphysiologie, Am Mühlenberg 1, 14476 Potsdam-Golm, Germany

⁴Department of Biochemistry, University of Wisconsin, Madison, WI 53706, USA

⁵Institute of Science and Technology (IST Austria), Am Campus 1, 3400 Klosterneuburg, Austria

⁶Institute of Biotechnology (IBT), University of Vilnius, V. Graiciuno 8, 02242 Vilnius, Lithuania

⁷Laboratory of Cell Biology, Wageningen University, Droeendaalsesteeg 1, 6708PB Wageningen, The Netherlands

⁸Department of Medical Protein Research, VIB, A. Baertsoenkaai 3, 9000 Ghent, Belgium

⁹Department of Biochemistry, Ghent University, 9000 Ghent, Belgium

¹⁰Department of Biology, Center for Proteome Analysis and Mass Spectrometry, University of Antwerp, 2020 Antwerp, Belgium

¹¹Flemish Institute for Technological Research (VITO), 2400 Mol, Belgium

¹²These authors contributed equally to this work

¹³Co-senior authors

*Correspondence: daniel.vandamme@psb.vib-ugent.be (D.V.D.), persson@mpimp-golm.mpg.de (S.P.)

<http://dx.doi.org/10.1016/j.cell.2014.01.039>

SUMMARY

Clathrin-mediated endocytosis is the major mechanism for eukaryotic plasma membrane-based proteome turn-over. In plants, clathrin-mediated endocytosis is essential for physiology and development, but the identification and organization of the machinery operating this process remains largely obscure. Here, we identified an eight-core-component protein complex, the TPLATE complex, essential for plant growth via its role as major adaptor module for clathrin-mediated endocytosis. This complex consists of evolutionarily unique proteins that associate closely with core endocytic elements. The TPLATE complex is recruited as dynamic foci at the plasma membrane preceding recruitment of adaptor protein complex 2, clathrin, and dynamin-related proteins. Reduced function of different complex components severely impaired internalization of assorted endocytic cargoes, demonstrating its pivotal role in clathrin-mediated endocytosis. Taken together, the TPLATE complex is an early endocytic module representing a unique evolutionary plant adaptation of the canonical eukaryotic pathway for clathrin-mediated endocytosis.

INTRODUCTION

The plasma membrane (PM) forms a fundamental barrier of the cell to communicate with the outside world. Plant cells can remove and add receptors, channels, and other membrane proteins in response to endogenous stimuli such as hormones (Du et al., 2013; Irani et al., 2012; Marhavý et al., 2011; Robert et al., 2010; Sutter et al., 2007), nutrient availability (Barberon et al., 2011; Takano et al., 2010), and pathogen defense (Bar et al., 2009; Robatzek et al., 2006). The process by which membrane materials and extracellular cargoes are internalized is called endocytosis (McMahon and Boucrot, 2011). Clathrin-mediated endocytosis (CME) is the best-characterized endocytic pathway in eukaryotes and is defined by the involvement of the vesicle coat scaffold protein clathrin.

CME requires a series of highly coordinated steps consisting of nucleation, cargo selection, vesicle coat assembly, scission, and vesicle uncoating (McMahon and Boucrot, 2011). The heterotetrameric adaptor protein complex 2 (AP2) represents the core complex for CME in animal cells. Here, clathrin-coated pit nucleation at the PM is hallmarked by the arrival of a clathrin triskelion in association with two AP2 complexes in a phosphatidylinositol 4,5-bisphosphate PI_(4,5)-P₂-dependent manner. This priming complex subsequently recruits more AP2-clathrin complexes and adaptor proteins required for clathrin coat stabilization (Cocucci et al., 2012; Henne et al., 2010; Kukulski et al., 2012). Among these adaptor elements, the muniscin proteins, complexed with intersectin, epsin, and EGFR pathway

substrate 15 (Eps15) proteins (Henne et al., 2010; Mayers et al., 2013; Reider et al., 2009) associate to the rim of the assembling coat (Tebar et al., 1996), where they are believed to stabilize bilayer curvature (Cocucci et al., 2012). Budding and eventual scission of the nascent vesicle depends on the enzyme activity of the GTPase dynamin. After detachment, the vesicle is uncoated to allow fusion with endosomal compartments. The cargo then traffics further within the endomembrane system and the endocytic machinery can be recycled (McMahon and Boucrot, 2011).

Many aspects of CME are evolutionarily conserved as can be inferred from the presence of obvious homologs of several CME effectors in plant, animal, and yeast genomes. However, important kingdom-specific modifications are also evident. Strikingly, AP2, muniscins, and dynamin are crucial for cargo selection and vesicle scission in human or zebrafish cells (Cocucci et al., 2012; Henne et al., 2010; Macia et al., 2006; Umasankar et al., 2012), but some are dispensable in yeast or worm (Mayers et al., 2013; Smaczynska-de Rooij et al., 2010; Yeung et al., 1999). On the other hand, CME in yeast depends strongly on actin dynamics, while the actin cytoskeleton is only required for CME in animal cells under high turgor pressure (Mooren et al., 2012). This implies that important features of CME have diverged significantly during evolution.

In plants, several evolutionarily conserved CME components can be recognized (Chen et al., 2011), including clathrin (Dhokshhe et al., 2007; Kitakura et al., 2011; Wang et al., 2013), the actin cytoskeleton (Nagawa et al., 2012), dynamin-related proteins (DRP) (Boutté et al., 2010; Collings et al., 2008; Fujimoto et al., 2010; Konopka et al., 2008), and adaptor proteins (Bar et al., 2008; Barth and Holstein, 2004; Lam et al., 2001; Song et al., 2012). While this indicates similarity to yeast and animal endocytosis, a broad range of animal- or yeast-like adaptor and accessory proteins are absent from plants, suggesting a profound divergence in eukaryote CME (Chen et al., 2011).

We previously identified TPLATE as a plant-specific interactor of clathrin, suggesting a CME-related function (Van Damme et al., 2011). Here, we show that TPLATE is part of a unique multi-subunit protein complex (the TPLATE complex, TPC) that acts in concert with the AP2 complex, dynamin-related proteins and clathrin, and that the complex is essential for plant survival. The early TPC recruitment to endocytic foci, the lack of clear yeast and animal homologs, and a requirement of the complex for CME support the hypothesis that the TPC represents an evolutionary modification of early-adaptor function for CME in plants.

RESULTS

The Multisubunit TPC Is Connected to CME Machinery

Previously, we identified TPLATE as a plant-specific protein with a similar developmental mutant phenotype as the *Arabidopsis* dynamin *dtp1c*. Copurification with clathrin furthermore suggested that TPLATE functions in membrane trafficking (Backeas et al., 2010; Van Damme et al., 2006; Van Damme et al., 2011). Clathrin coats are abundant at the plant trans-Golgi Network/early endosome (TGN/EE), as well as at the PM (Konopka et al., 2008). In interphase *Arabidopsis* root cells, clathrin light

chain2 (CLC2) and TPLATE only colocalized at the PM (Figure 1A), which favors a role for TPLATE in clathrin-dependent processes occurring at the PM, rather than at the TGN/EE.

We used tandem affinity purification (TAP) experiments in PSB-D *Arabidopsis* suspension-cultured cells to identify putative TPLATE interactors. Four independent TAP experiments with TPLATE as bait reproducibly identified seven interacting proteins of unknown function with molecular weights (MW) ranging from 17 kDa to 176 kDa. We named these TASH3, AtEH1, AtEH2, LOLITA, TML, TWD40-1, and TWD40-2 based on the presence of specific protein domains (Figure S1A and Tables S1, S2, S3 available online). An in silico comparison of all TPC subunits against human and yeast genomes showed that the TPC subunits have no obvious counterparts in those kingdoms, although they likely share a common evolutionary origin with trafficking proteins (Table S1).

A total of 28 reverse TAP experiments using these seven TPLATE prey proteins as baits reciprocally recovered all eight interactors with very high efficiency (Figure 1B; Tables S2 and S3), suggesting that they represent a stable complex of eight core components, which we named the TPLATE complex (TPC). Two-dimensional (2D) Blue-Native/SDS-PAGE revealed that both TPLATE and TML appeared as monomers and incorporated into larger protein complexes of various sizes up to approximately 800 kDa (Figure S1B). Without posttranslational modifications, the combined molecular mass of the eight subunits in the TPC complex identified by chromatography was estimated to be 918 kDa (Table S1), which corresponds well with the 2D-PAGE observations. The range of complex sizes might reflect different stages of complex assembly/disassembly or complex degradation during extraction and/or gel separation.

Furthermore, coimmunoprecipitation (coIP) experiments (Figure S1C), yeast two hybrid experiments (Y2H) and bimolecular fluorescence complementation (BiFC) assays (Figures S1D and S1E) independently confirmed interactions between several of the subunits of this complex. The reverse TAP experiments also revealed a link between the TPC and members of the dynamin protein family (DRP1A, DRP1C, DRP1E, DRP2A, and DRP2B) and the small (AP2S) and alpha1 (AP2A1) subunits of the *Arabidopsis* AP2 Adaptor protein complex (Di Rubbo et al., 2013; Yamaoka et al., 2013). Subsequent TAP experiments in cell suspensions using clathrin heavy chain1 (CHC1) as bait revealed additional interactions with other subunits of the clathrin scaffold (Figure 1B; Tables S2 and S3). In addition, affinity-purification experiments using functional TPLATE-GFP or TML-YFP followed by mass spectrometry analysis (APMS) and by western blotting (coIP) confirmed the composition of the TPC in planta and its relation with DRPs, CLCs, CHCs, and AP2. Moreover, these APMS experiments identified two proteins containing an AP180 N-terminal homology (ANTH) domain (AtECA4 and CAP1; Figures 1B, 1C, and S1A; Tables S1, S2, and S3). Notably, in silico searches revealed putative clathrin-binding boxes, AP2 complex recognition motifs, and sorting motifs in many subunits of the TPC (Figure S1A).

Taken together, we demonstrate that TPLATE assembles into a robust multimeric protein complex that physically interacts with DRPs, AP2 complex subunits, ANTH domain-containing proteins, and clathrins, supporting its involvement in CME.

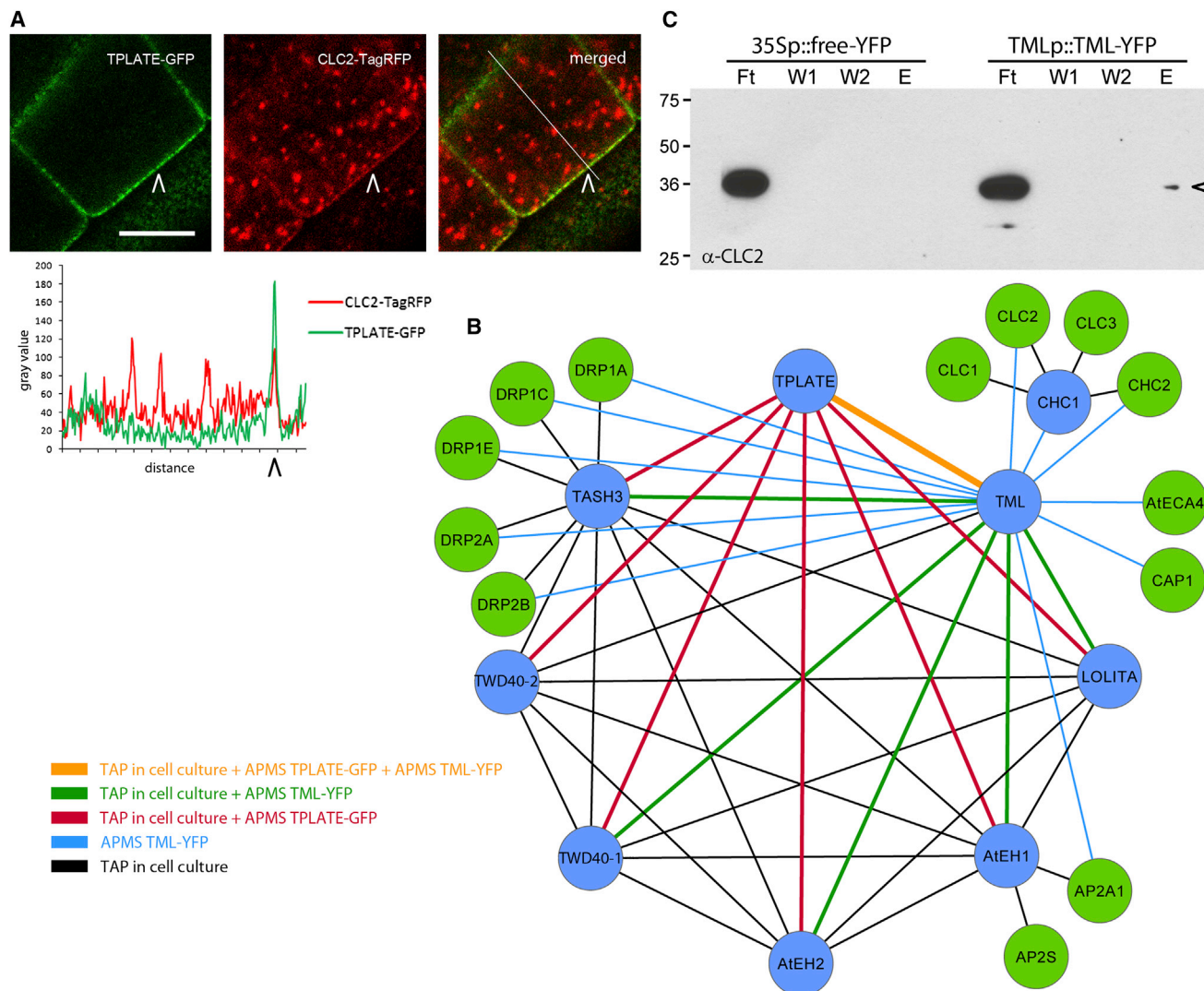


Figure 1. TPLATE Is Part of a Multisubunit Protein Complex That Connects Key Components of Clathrin-Mediated Endocytosis

(A) Confocal images of *Arabidopsis* root epidermal cells and corresponding line plot showing colocalization of TPLATE and CLC2 at the PM (arrowheads). (B) Spoke-model interaction network of the identified protein complex. Proteins share cocomplex membership with their interactors through direct or indirect binding. The color coding of the connecting lines corresponds to the experiments listed. Blue nodes represent bait proteins for TAP-tag and APMS experiments, green nodes represent prey proteins. (C) colP confirmation of the interaction between TML and CLC2. Endogenous CLC2 copurified with TML-YFP in the eluted fraction (E, arrowhead) in contrast with the control experiment. CLC2 was also detected in the flow through (Ft), but not in the wash fractions (W1 and W2). Scale bar, 10 μ m. See also Figure S1, Table S1, S2 and S3.

The TPC Functions at the PM and Is Required for Pollen Development

Similar to the *tplate*, *clc1*, and *drp1c* mutants (Backues et al., 2010; Van Damme et al., 2006; Wang et al., 2013), which function in CME and produce unviable pollen grains, mutants in four newly identified TPC subunits displayed a fully penetrant pollen defect causing male sterility. Six mutant alleles of four subunits of the TPC showed failure in male transmission of the mutation (Figure S2A; Table 1). In agreement with an essential role of these proteins for pollen development, these phenotypes also correlated with the occurrence of shriveled and normal pollen in a

1:1 ratio revealed by scanning electron microscopy analysis (Figures 2A and S2B). In contrast, female transmission of the mutation occurred normally or with slightly decreased ratios (Table 1).

All subunits of the identified complex localized exclusively to the PM in *Arabidopsis* root cells (Figure S2C). Moreover, expression of fluorescent fusion protein-tagged forms of TML (TML-FFP) under control of its endogenous promoter rescued the male transmission failure of both *tml-1* and *tml-2* mutant alleles (Table 1), demonstrating that TML-FFP is functional. Confocal microscopy revealed recruitment of TML fusions to the PM and the growing cell plate in *Arabidopsis* root cells (Figures 2B, 2C,

Table 1. Segregation Analysis of Mutants in TPC Subunits

Line	Insertion	Total	WT	Heterozygous	Homozygous	Ratio	χ^2
Segregation Analysis							
<i>tml-1(+/-)</i>	GK_088H05	91	49	42	0	1:1	0.54
<i>tml-2(+/-)</i>	SALK_071882	102	53	49	0	1:1	0.16
<i>tml-1(+/-) + TMLp::TML-GFP(+/-)</i>	GK_088H05	81	n.a.*	63	18	3:1	0.33
<i>tml-2(+/-) + TMLp::TML-YFP(+/+)</i>	SALK_071882	52	12	27	13	1:2:1	0.12
<i>ateh2-1(+/-)</i>	SALK_092023	137	108	29	0	<1:1	n.a.
<i>twd40-1-1(+/-)</i>	SALK_121332	144	71	73	0	1:1	0.03
<i>twd40-2-1(+/-)</i>	GABI_776E02	93	47	46	0	1:1	0.01
<i>twd40-2-2(+/-)</i>	SALK_121649	98	51	47	0	1:1	0.16
Backcross Segregation Analysis WT♀ x Mutant♂							
<i>tml-1(+/-)</i>	GK_088H05	110	110	0		1:0	0.00
<i>tml-2(+/-)</i>	SALK_071882	100	100	0		1:0	0.00
<i>ateh2-1(+/-)</i>	SALK_092023	81	81	0		1:0	0.00
<i>twd40-1-1(+/-)</i>	SALK_121332	96	96	0		1:0	0.00
<i>twd40-2-1(+/-)</i>	GABI_776E02	254	254	0		1:0	0.00
<i>twd40-2-2(+/-)</i>	SALK_121649	130	130	0		1:0	0.00
Backcross Segregation Analysis WT♂ x Mutant♀							
<i>tml-1(+/-)</i>	GK_088H05	142	78	64		1:1	1.38
<i>tml-2(+/-)</i>	SALK_071882	102	52	50		1:1	0.06
<i>ateh2-1(+/-)</i>	SALK_092023	218	164	54		<1:1	n.a.
<i>twd40-1-1(+/-)</i>	SALK_121332	90	47	43		1:1	0.18
<i>twd40-2-1(+/-)</i>	GABI_776E02	286	153	133		1:1	1.40
<i>twd40-2-2(+/-)</i>	SALK_121649	106	72	34		<1:1	n.a.

Segregation ratios of the progeny of heterozygous mutants, complemented mutants and backcrosses to wild-type (Col-0) are shown. All tested alleles in TPC subunits result in fully penetrant male sterility as the T-DNA could not be transferred to the next generation using the heterozygous mutant plants as pollen donor in contrast to backcrosses using wild-type (WT, Col-0) pollen. Expression of TML C-terminal fusion constructs driven by endogenous promoter sequences complements both mutant alleles. The lower female T-DNA transmission rates for *ateh2-1* and *twd40-2-2* point to additional effects on the female gametophyte. n.a., not applicable. n.a.*, not applicable as wild-type seedlings were omitted from the analysis by antibiotic selection prior to genotyping. Chi square (χ^2) values for the observed segregation ratios are indicated where applicable.

and 2F), to the pollen tube exit site (Figure 2D), and to the shank of growing pollen tubes while being excluded from the very tip (Figure 2E). These localizations are in agreement with previous reports on TPLATE and DRP localizations (Konopka et al., 2008; Van Damme et al., 2006; Van Damme et al., 2011). Furthermore, the identical localizations and mutant phenotypes of individual TPC subunits strongly confirm our proteomics data of a single multimeric protein complex.

The TML subunit has a μ homology domain (μ HD) in its C terminus (Table S1; Figure S1A) that generally is involved in membrane interactions, cargo recognition, and binding and recruitment of accessory proteins (McMahon and Boucrot, 2011). In contrast to full-length TML, truncating the μ HD (TML Δ C) or expression of the C-terminal part of this domain (GFP-CtermTML) resulted in cytoplasmic localization (Figures 2F–2I). Furthermore, APMS experiments using TML Δ C as bait could not recover certain TPC core components (Figure S2D; Tables S2 and S3) and caused a reduction in TPC complex size (Figure S2E), suggesting that an intact μ HD of TML is required for PM recruitment and for full TPC assembly.

The μ HD is a common feature of adaptor proteins such as the medium subunit adaptins (AP1 to 5), the cargo-specific stonins,

delta COPI proteins, the SH3-containing GRB2-like protein 3-interacting protein 1 (SGIP1), suppressor of yeast profilin 1 (SYP1), and FCH domain-only (FCHo) proteins. We performed an extensive phylogenetic analysis of all above-mentioned protein families encoded in human, yeast, *Arabidopsis*, and a set of evolutionarily diverse plant species. For all major classes of APs, plant, yeast, and animal homologs clustered together, while TML and its homologs clustered with the muniscin proteins SGIP1 and FCHo/SYP1 (Reider et al., 2009) (Figures 2J and S2F), further suggesting that the TML containing TPC functions as an early endocytic adaptor complex in plants.

TPC Recruitment at the PM Is an Early Event of CME

Typically, CME is characterized by dynamic recruitment and assembly of different effector proteins at the PM (Boettner et al., 2012; Cocucci et al., 2012; Henne et al., 2010; McMahon and Boucrot, 2011). The close proteomic relationship of TPC components with the core CME machinery, and the PM localization of these proteins, prompted us to characterize their dynamic localization at the PM (Figures 3A and S3). Similar to AP2A1-GFP and CLC2-mORANGE, TPC components including TPLATE-, TML-, AtEH1-, AtEH2-, LOLITA-, and TASH3-GFP dynamically

appeared and disappeared as discrete foci which did not show any lateral mobility (Figures 3A and S3; Movie S1).

Quantification of the dynamic behavior of TPLATE-, TML-, and AP2A1-positive foci showed that they had comparable average dwell times at the PM ranging between 7 and 38 s (Figure 3B). Consistent with a function in a common process, TML-positive foci showed a high degree of colocalization with both CLC2 and DRP1C (~70% and ~80% respectively, Figures 3C and 3D). In nearly all of the colocalizing foci, TML was recruited to the PM earlier than or concomitant with CLC2 (Figures 3C and 3D; Movie S2). DRP1C, which has a late function in CME (Fujimoto et al., 2010; Konopka et al., 2008), was consistently recruited late to the TML-positive foci (Figures 3C and 3D; Movie S3). These observations suggest that recruitment of the TPC to the PM marks early events of CME in plants.

The TPC Functions in Concert with AP2 during Early CME

During CME in higher eukaryotes, the heterotetrameric AP2 complex is essential for cargo recognition and initiation of coat formation via clathrin recruitment to the PM (Cocucci et al., 2012; Collins et al., 2002). Our proteomics approach linked several members of the TPC with AP2A1 and AP2S, two subunits of the *Arabidopsis* heterotetrameric AP2 complex (Di Rubbo et al., 2013; Yamaoka et al., 2013). In addition, AP2A1 showed similar dynamic behavior as TPC subunits (Figures 3A and 3B; Movie S1), it colocalized exclusively at the PM with TPLATE and TML, and AP2A specifically coimmunoprecipitated with TPLATE (Figures S4A and S4B).

To further elucidate the relationship between AP2 and the TPC, we visualized their dynamic behavior at the PM (Figures 4A, 4B, S4C, and S4D; Movies S4 and S5). The majority of the fluorescent foci containing TPLATE and TML colocalized with AP2A1. A time-course analysis of the dynamic behavior of these foci followed by time-projection of the individual frames exceeding the average life-times of the foci at the PM ($t = 50$ s), revealed the occurrence of three different populations of dynamic foci. Roughly 50% of foci showed colocalization between TPLATE/TML and AP2A1. In addition, two populations of foci occurred that only recruited either TPLATE/TML (~30%) or AP2A1 (~20%; Figure 4C). Both TPLATE and TML colocalized with AP2A1 with similar ratios, consistent with their function in a common complex. The occurrence of these three populations of endocytic foci suggests that the TPC and AP2 have overlapping, but also distinct functions. To establish the order of recruitment between the different complexes, we performed a detailed analysis of those foci that acquired both TPLATE/TML and AP2A1. We found a strong, yet not exclusive tendency for TPC subunits to arrive at the PM prior to AP2 and to remain present after AP2 removal by vesicle scission (Figures S4C and S4D).

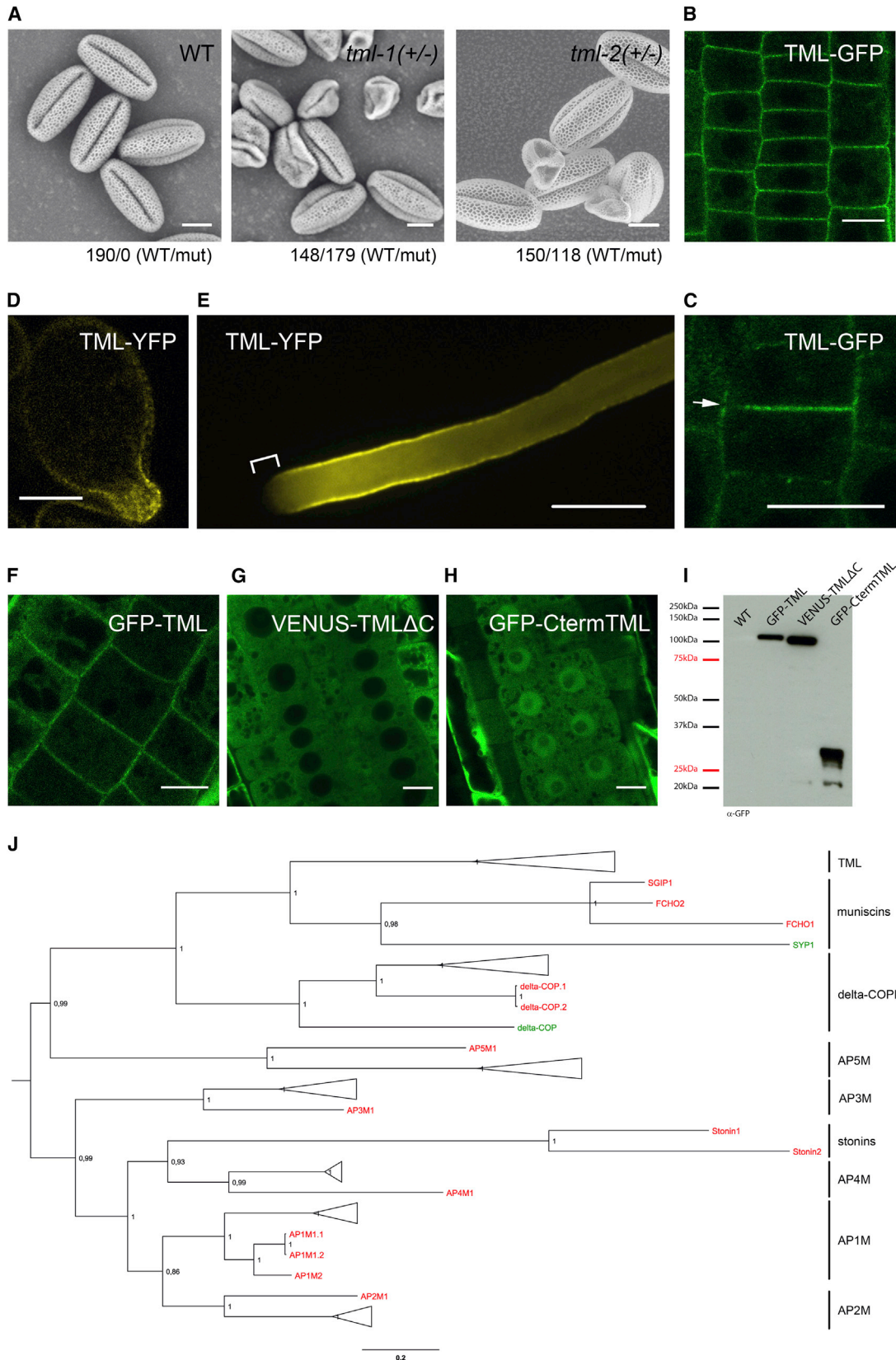
Together, these data support the idea that the TPC acts as an early modulator of CME in concert with AP2.

Endocytosis at the PM Requires a Functional TPC

The recruitment of TPC subunits to endocytic foci at the PM, together with the male gametophytic phenotype, suggests a pivotal function for this complex in CME but the lethal phenotype also inhibits any functional genetic approach. We therefore used

an artificial micro RNA (amiR)-based silencing approach (Schwab et al., 2006) to unravel the somatic function of this complex. Constitutive silencing using amiR constructs directed against *TPLATE* or *TML* (*amiR-TPLATE* and *amiR-TML*) resulted in poorly developing seedlings that died before forming true leaves. This phenotype correlated with a substantial reduction of *TPLATE* or *TML* mRNA levels (Figures S5A and S5B) and corroborates that the TPC proteins are essential for plant survival. Notably, the transcript level for the medium subunit of the *Arabidopsis* C-terminal μ HD-containing AP2 complex subunit AP2M was upregulated in *amiR-TML* seedlings (Figure S5B), excluding unspecific silencing of *AP2M*. To investigate whether constitutive knockdown of *TML* and *TPLATE* in seedlings impaired endocytosis, we used the endocytic tracer FM4-64. In wild-type *Arabidopsis* roots, a short-term FM4-64 pulse labels the PM and subsequently early endosomes on its way to the vacuole (Dettmer et al., 2006). In contrast, in seedlings expressing the *amiR-TPLATE* or *amiR-TML*, uptake of FM4-64 from the PM into endosomes was strongly inhibited (Figures S5A and S5B). The endocytic defect was visualized more prominently by application of the fungal toxin Brefeldin A (BFA), which aggregates early endosomes (TGN/EE) in so-called BFA bodies and blocks recycling of internalized membrane to the PM (Geldner et al., 2003). As a consequence, endocytosed material becomes trapped in the aggregated TGN/EE (Dettmer et al., 2006; Geldner et al., 2003; Grebe et al., 2003). Quantification of both BFA body distribution and FM4-64 fluorescence intensity showed a clear reduction both in the amount of BFA bodies and in dye accumulation in roots expressing *amiR-TML* as compared to wild-type (Figure S5C).

The seedling lethality of constitutive silencing was overcome by expressing the *amiR-TML* and *amiR-TPLATE* under an estradiol inducible promoter (Curtis and Grossniklaus, 2003). Estradiol-induced expression of *amiR-TML* and *amiR-TPLATE* substantially reduced mRNA levels of both genes and caused severe seedling growth retardation, decreased root apical meristem size, bulging of root epidermal cells that reflect defective root hair morphogenesis (Figures S5D–S5G), and ultimately seedling lethality. We also observed defects in graviperception compared to control lines or lines grown without induction (Figure S5H) and block of FM4-64 uptake in root cells (Figure S5I) as observed with the constitutively silenced lines. Following BFA treatment, FM4-64 prominently decorated BFA-bodies in control lines, while only a very faint internalized FM4-64 signal could be detected in the induced *amiR-TML* lines (Figure 5A). To investigate a more general role for the TPC in CME, we examined the trafficking of a GFP-tagged form of the brassinosteroid (BR) receptor, BR insensitive1 (BRI1) in inducible *amiR-TML* lines. BRI1-GFP cycles constitutively between the PM and TGN/EE (Geldner et al., 2007), and its internalization depends on clathrin (Irani et al., 2012). Consistent with a broad CME-related function of the TPC, the induction of *amiR-TML* correlated with an increased BRI1-GFP labeling of the PM compared to control seedlings (Figure 5A and 5B). The endosomal aggregation of BRI1 furthermore demonstrated that the BFA effect was not impaired after induction of the *amiR-TML* (Figure 5A). This corroborates that the reduced labeling of BFA bodies by FM4-64 in the induced *amiR-TML* seedlings was due to a defect in



(legend on next page)

endocytic uptake of the dye, and thus highlighted a general defect in endocytosis.

In addition, the recently reported AlexaFluor 647-coupled castasterone (AFCS), which acts as a ligand of BRI1, readily labeled the vacuolar lumen in control seedlings, but did not internalize in estradiol-induced *amiR-TML* cells (Figure 5C). Taken together, the enhanced PM accumulation of BRI1 and the inhibition of AFCS uptake in *amiR-TML* lines are in agreement with defective endocytosis of BRI1 (Irani et al., 2012) upon downregulation of *TML* expression. Silencing of *TML* also reduced the accumulation of endogenous AP2A at the PM and forming cell plates (Figure 5D) which links the observed BRI1 and AFCS internalization defects in the *amiR-TML* seedlings to the AP2-dependent internalization of BRI1 and AFCS (Di Rubbo et al., 2013).

The polarly localized auxin transport proteins PIN1 and PIN2 (Petrásek et al., 2006) are internalized via CME (Kitakura et al., 2011) and their endocytic dynamics can be readily visualized by BFA treatment (Dhonukshe et al., 2007; Geldner et al., 2001; Tanaka et al., 2009). In agreement with a general function for the TPC in CME, the accumulation of internalized PIN1 and PIN2 in BFA bodies was severely reduced in induced *amiR-TML* seedlings compared to controls (Figure 5E and 5F).

Another reported defect caused by general inhibition of both clathrin and dynamin function is the ectopic accumulation of the cytokinesis-specific syntaxin KNOLLE at the PM and cortical division zone (Boutté et al., 2010). Consistent with a general defect in CME, we found that many recently divided cells in induced *amiR-TML* roots showed ectopic KNOLLE localization, while such patterns were rarely observed in control roots (Figure 5G and 5H).

In summary, the alteration in internalization and localization of several well-established cargoes of CME highlights the TPC as an essential novel regulator of early events of CME. This notion is further supported by the observation that silencing of *TML* results in a lower abundance of AP2A at the PM and cell plates.

DISCUSSION

CME is the most prominent mode of endocytic cargo internalization in higher eukaryotes (Boettner et al., 2012; Chen et al., 2011; McMahon and Boucrot, 2011). While the overall mechanism of CME and many of its molecular components appear evolutionarily conserved in eukaryotes (Boettner et al., 2012; Conibear,

2010), different proteins and cargo recognition strategies are also evident. Hence, to grant a deeper understanding of CME and its evolution, it is necessary to identify the functional CME constituents in different eukaryotic kingdoms.

Here, we report the identification of the TPLATE complex consisting of eight core components that drives CME in the model plant *Arabidopsis*. This complex is comprised of the previously identified plant-specific adaptor protein TPLATE (Van Damme et al., 2006; Van Damme et al., 2011) as well as seven previously uncharacterized proteins (Figure 6). Notably, we found that the TPC subunits physically and genetically interact with multiple conserved CME regulators (Backues et al., 2010; Kang et al., 2003; Wang et al., 2013), showed dynamic recruitment to foci at the PM with similar average dwell times as AP2, clathrin, and dynamin proteins (Konopka et al., 2008) and are required for endocytosis of diverse cargo proteins and endocytic tracers. While our data clearly points to the existence of a high molecular weight protein complex containing the eight identified subunits and associated components and a role of the μ HD of *TML* in full TPC complex assembly, specific intermolecular relationships and the exact spatio-temporal formation of this complex still remain to be unraveled.

TPC Functions in Concert with AP2 at the PM

Although several of the TPC components contain domains present in yeast and animal CME adaptors, the protein components of the TPC do not have any obvious homologs in yeast and animals, supporting the notion that adaptor-related proteins have substantially diverged during evolution (Chen et al., 2011). With the exception of AteH1 and AteH2, not a single hit could be identified for any TPC subunit in these model species at a more stringent E-value cutoff of e^{-10} , indicating that the identified complex is plant-specific. Nevertheless, the *in silico* analysis does show that TPC subunits likely share a common evolutionary origin with membrane trafficking proteins in other kingdoms. Notably, some TPC subunits have features reminiscent of an endocytic hub complex that contains FcHo, Eps15, and Intersectin, required to stabilize initial AP2 recruitment to the PM in animal cells (Cocucci et al., 2012; Henne et al., 2010; Mayers et al., 2013; Umasankar et al., 2012). *TML* is related to SYP1 and FcHo, suggesting a potential role for TMLs as muniscin-like adaptors in plants. Moreover, AteH1 and AteH2 contain an EH domain architecture and have Eps15Like-1 and Intersectin

Figure 2. TML Is a PM-Associated, Muniscin-like Protein

(A) SEM images of pollen from wild-type (WT, Col-0), *tml-1(+/-)*, and *tml-2(+/-)* showing formation of shriveled pollen in heterozygous *tml* mutants. Ratios of WT versus mutant pollen are indicated.
 (B–E) Localizations of functional TML-FFP. In complemented *Arabidopsis tml-1(-/-)* root cells, TML localizes at the PM (B), the forming cell plate, and the cortical division zone prior to cell plate anchoring (C, arrow). During pollen germination, TML in the complemented *tml-2(-/-)* background localizes to the pollen tube exit site at the onset of pollen tube formation (D) and at the lateral sides of a growing pollen tube while being absent at the very tip of the pollen tube (E, bracket; time projection $n = 100$ frames, $t = 200$ s).
 (F–H) TML requires an intact μ HD for PM recruitment. Full-length TML localizes to the PM (F), while a C-terminal truncated version (VENUS-TML Δ C, G) localizes to the cytoplasm. PM targeting does not rely on the C-terminal part of TML alone as a construct containing the C-terminal 73AA of TML (GFP-CtermTML, H) shows cytoplasmic and nuclear localization.
 (I) Anti-GFP western blot detecting GFP-TML, VENUS-TML Δ C, and the GFP-CtermTML at the appropriate sizes. WT (Col-0) served as control.
 (J) Phylogenetic analysis positioning TML among all protein families with a μ HD. Proteins from *Arabidopsis* and a set of evolutionarily diverse plant species (black), human (red), and baker's yeast (green) are depicted. The full tree depicting all proteins used can be found in Figure S2F. Additional reference numbers are listed in the extended experimental procedures. TML groups within the muniscin protein clade.
 The scale bar indicates the average number of substitutions per amino acid site. Scale bars, 10 μ m in (A)–(D) and (F)–(H) and 50 μ m in (E). See also Figure S2.

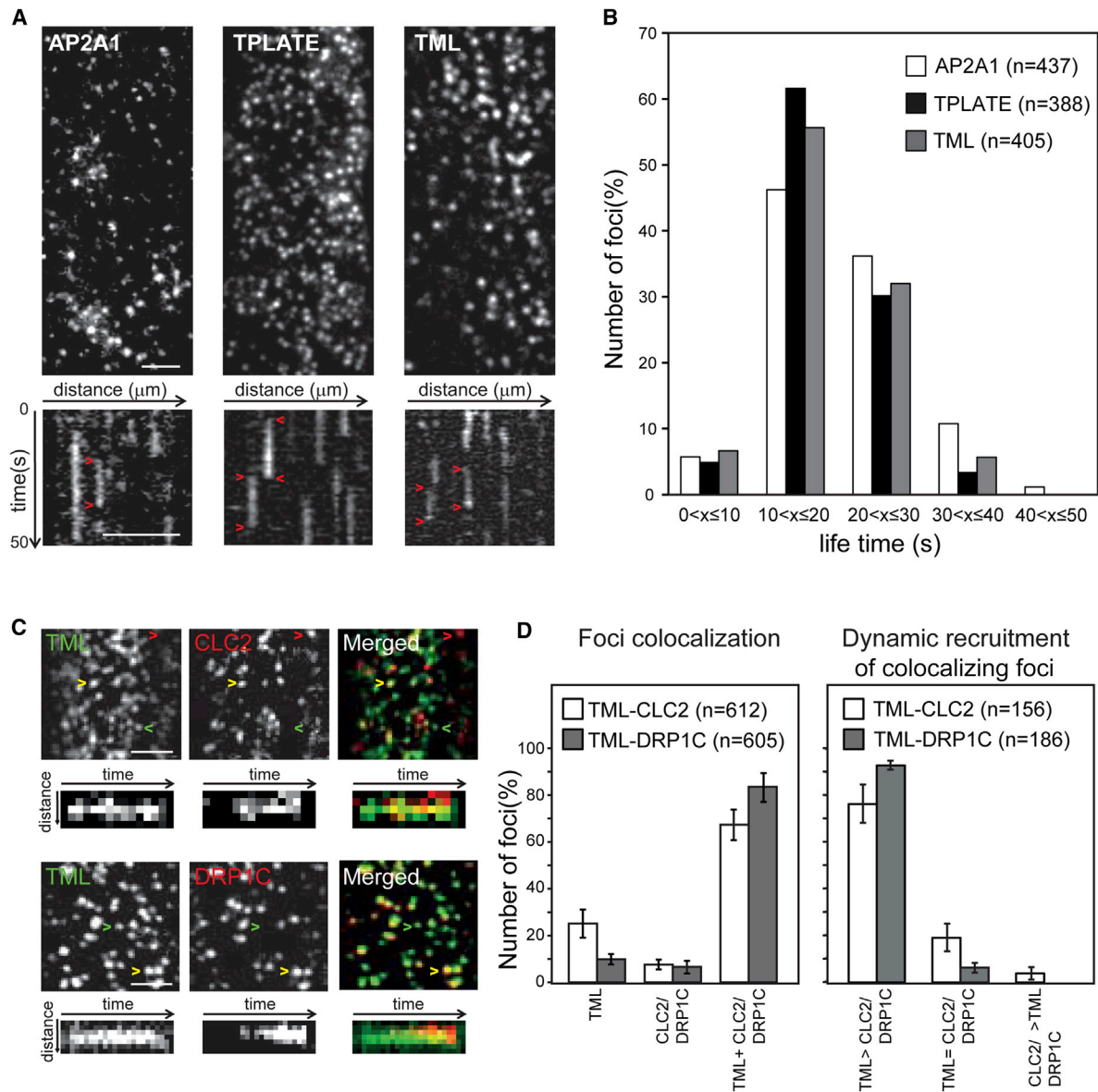


Figure 3. Several Subunits Link the Identified TPC to Clathrin-Mediated Endocytosis

(A) Representative VAEM/spinning disc images and kymographs of *Arabidopsis* hypocotyl epidermal cells taken from the corresponding movies (n = 50 frames, t = 50 s) showing recruitment of AP2A1, TPLATE, and TML in discrete and highly dynamic foci. Red arrowheads mark the dwell-time of the proteins at the PM. (B) Life-time measurements of the AP2A1, TPLATE, and TML foci. All three proteins share a similar life-time distribution with the majority of the foci having a life-time between 7 and 38 s.

(C) Spinning disc time projections (n = 15 frames, t = 15 s) of *Arabidopsis* hypocotyl cells expressing TML-YFP and CLC2-mOrange (top) or TML-YFP and DRP1C-mOrange (bottom). The majority of TML-containing foci recruit CLC2 and DRP1C during their life-time (yellow arrowheads), while only a few events contain only TML (green arrowheads) or CLC2/DRP1C (red arrowheads). Representative kymographs show TML recruitment preceding DRP1C recruitment and slightly preceding or concomitant with CLC2 recruitment.

(D) Quantification of the colocalization (left) and order of recruitment (right) of TML-CLC2 and TML-DRP1C. TML colocalizes strongly with the clathrin (CLC2) and the dynamin (DRP1) markers (left graph) and a significant percentage of foci show PM recruitment of TML prior to CLC2 and DRP1C (right graph). Error bars represent SEM. Scale bars, 5 μm . See also Figure S3 and Movies S1, S2, and S3.

1 as their closest human counterparts, while the TASH3 protein contains an SH3 domain, present in Intersectin but lacking in AtEH2. Therefore, a possible scenario may be that these subunits represent an AP2-recruiting unit in plant cells. Consistent

with this hypothesis, the AP2- and TPC-related proteins colocalized in dynamic endocytic foci at the PM in over 50% of all foci analyzed, and silencing of *TML* resulted in a lower abundance of AP2A at the PM and cell plates.

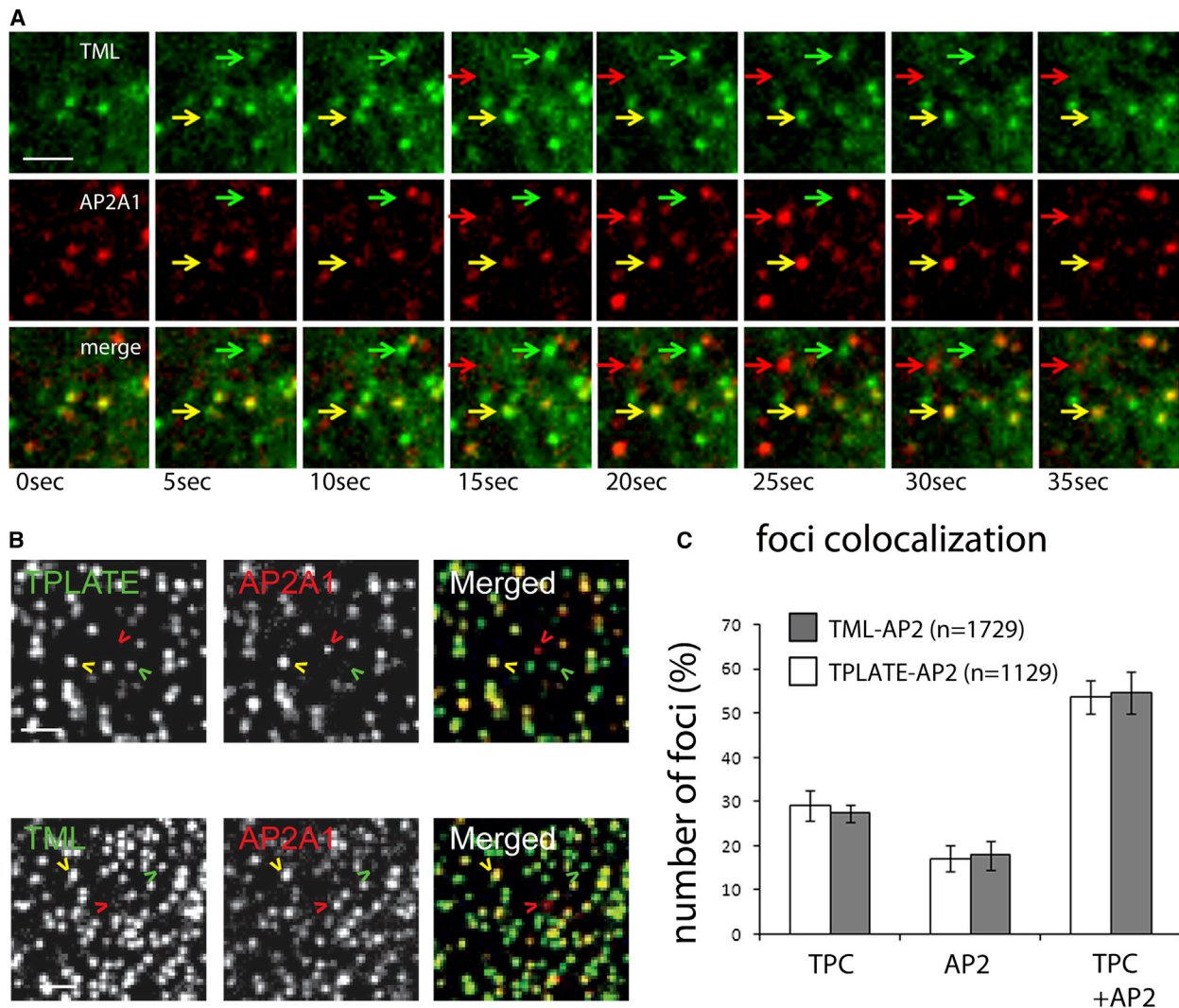


Figure 4. The TPC Functions in Concert with AP2

(A) Time series of a spinning disc movie (5 s/frame) showing the dynamic behavior of TML-GFP and AP2A1-TagRFP. Representative foci recruiting only TML (green arrows), TML and AP2A1 (yellow arrows), and only AP2A1 (red arrows) are indicated.

(B) Spinning disc time projection (n = 10 frames, t = 50 s) of *Arabidopsis* hypocotyl cells expressing TPLATE-GFP and AP2A1-TagRFP (top) or TML-GFP and AP2A1-TagRFP (bottom). Arrowheads indicate foci containing TPLATE only (green), TPLATE and AP2A1 (yellow), or AP2A1 only (red).

(C) Quantification of the number of foci from the time projections containing only the TPC (represented by TPLATE or TML), only AP2 (represented by AP2A1), or both complexes.

Error bars represent SEM. Scale bars represent 5 μ m. See also [Figure S4](#), [Movies S4](#) and [S5](#).

We further demonstrate that the arrival of TPC subunits at the PM in *Arabidopsis* epidermal cells preceded DRP, and AP2 in the majority of foci examined and slightly preceded, or was concomitant with, clathrin recruitment. This reveals the TPC as the earliest marker of plant CME. Moreover, TPC subunits typically remained at the PM after AP2 removal, possibly through scission of the endocytic vesicle, again reminiscent of the FCHO-Eps15-Intersectin rim complex that is excluded from the budded coated vesicle in animal cells (Cocucci et al., 2012). Consequently, the TPC behaves in a manner comparable to several well-defined yeast and animal CME regulators, despite the low degree of sequence homology between them.

While much of the AP2 and TPC proteins dynamically colocalized at the PM, we observed many dynamic endocytic spots labeled exclusively by the TPC, which might explain the persistence of dynamic clathrin foci at the PM in AP2 σ mutants (Fan et al., 2013). Although we did not analyze the dynamics of clathrin foci in TML or TPLATE silenced lines, we did find that TML silencing severely reduced PM recruitment of AP2A, suggesting that the TPC could be important to stabilize AP2 at the PM in the foci where AP2 and TPC co-occur.

Also, a minor fraction of foci only recruited AP2 subunits, suggesting that the TPC and AP2 can also exist independently, and if certain subunits of the TPC can recruit or stabilize AP2 at the PM,

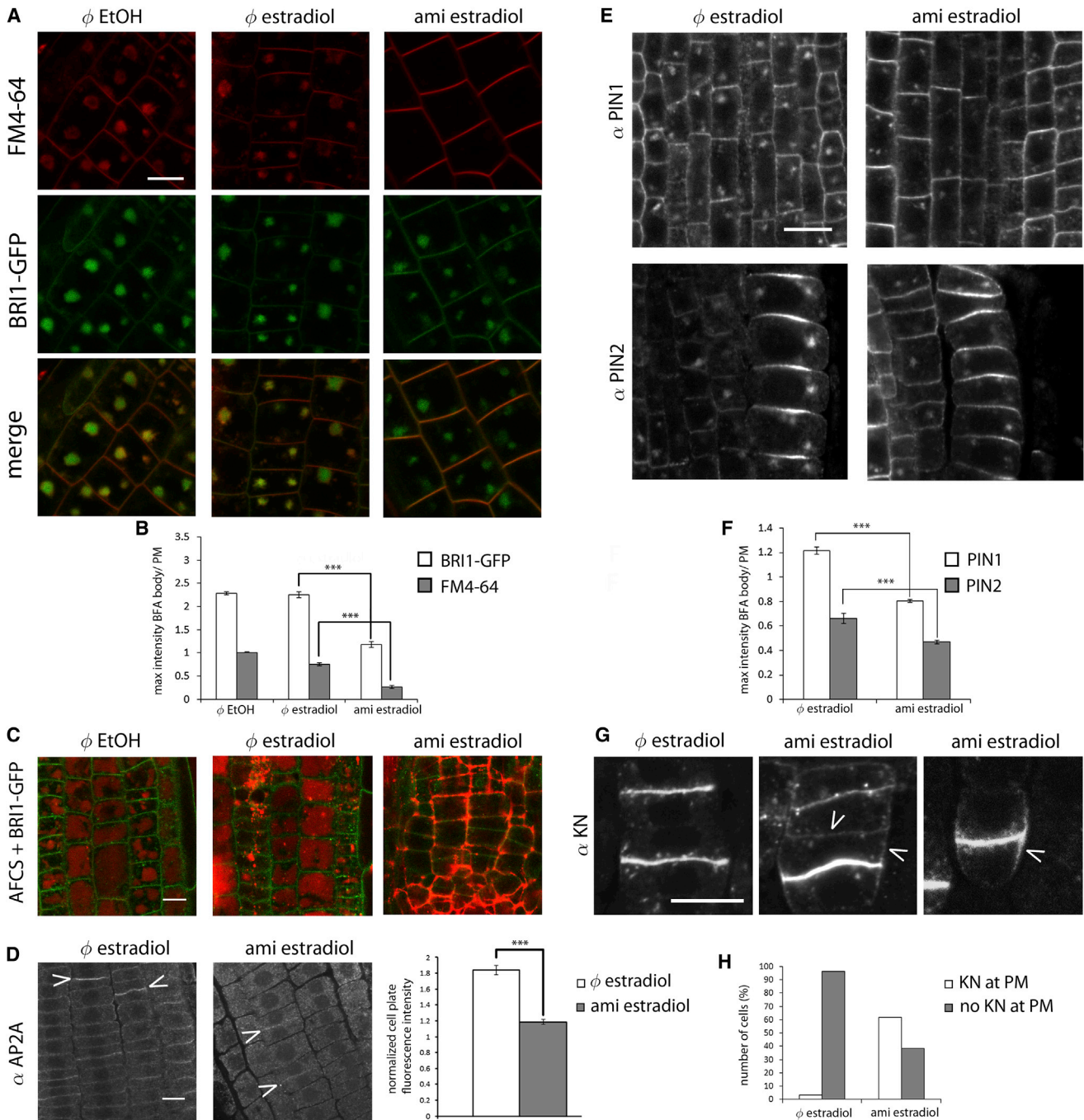


Figure 5. Silencing of TML Impairs Endocytosis of Several Cargo Proteins

(A) Representative images of *Arabidopsis* root cells expressing pBRI1::BRI1-GFP grown on control (ϕ EtOH) medium or on 5 μ M beta-estradiol (ϕ estradiol) and seedlings expressing pBRI1::BRI1-GFP and pESTR::amiR-TML on 5 μ M beta-estradiol (ami estradiol). Seedlings were treated with BFA (50 μ M; 1 hr) and stained with FM4-64 (4 μ M; 10 min). Induction of *amiR-TML* blocks accumulation of FM4-64 and reduces the accumulation of BRI1 in BFA bodies.

(B) Quantification of the experiment in (A). Both BRI1-GFP and FM4-64 accumulation is strongly reduced upon induction of *amiR-TML* (Student's t test p value < 0.0001, triple asterisk; n = 123 for ϕ EtOH, 3 roots; n = 115 for ϕ estradiol, 5 roots; n = 116 for ami estradiol, 4 roots).

(C) AFCS uptake experiment in pBRI1::BRI1-GFP expressing seedlings without (ϕ EtOH and ϕ estradiol) and with induction of *amiR-TML* (ami estradiol). AFCS accumulation in the vacuole (red) is blocked upon *amiR-TML* induction, in contrast to the control experiments.

(D) Representative immunolocalizations using an AP2A specific antibody (α AP2A) between control (pBRI1::BRI1-GFP, ϕ estradiol) and *amiR-TML* expressing lines (ami estradiol) showing reduced membrane recruitment of AP2A upon silencing *TML* (arrowheads). The graph shows the quantification of the ratio of cell plate fluorescence normalized to cytoplasmic signal with a clear reduction of membrane-associated AP2A upon silencing *TML* (Student's t test; p value < 0.0001, triple asterisk; ϕ estradiol, n = 37, 8 roots; ami estradiol, n = 46, 12 roots).

(legend continued on next page)

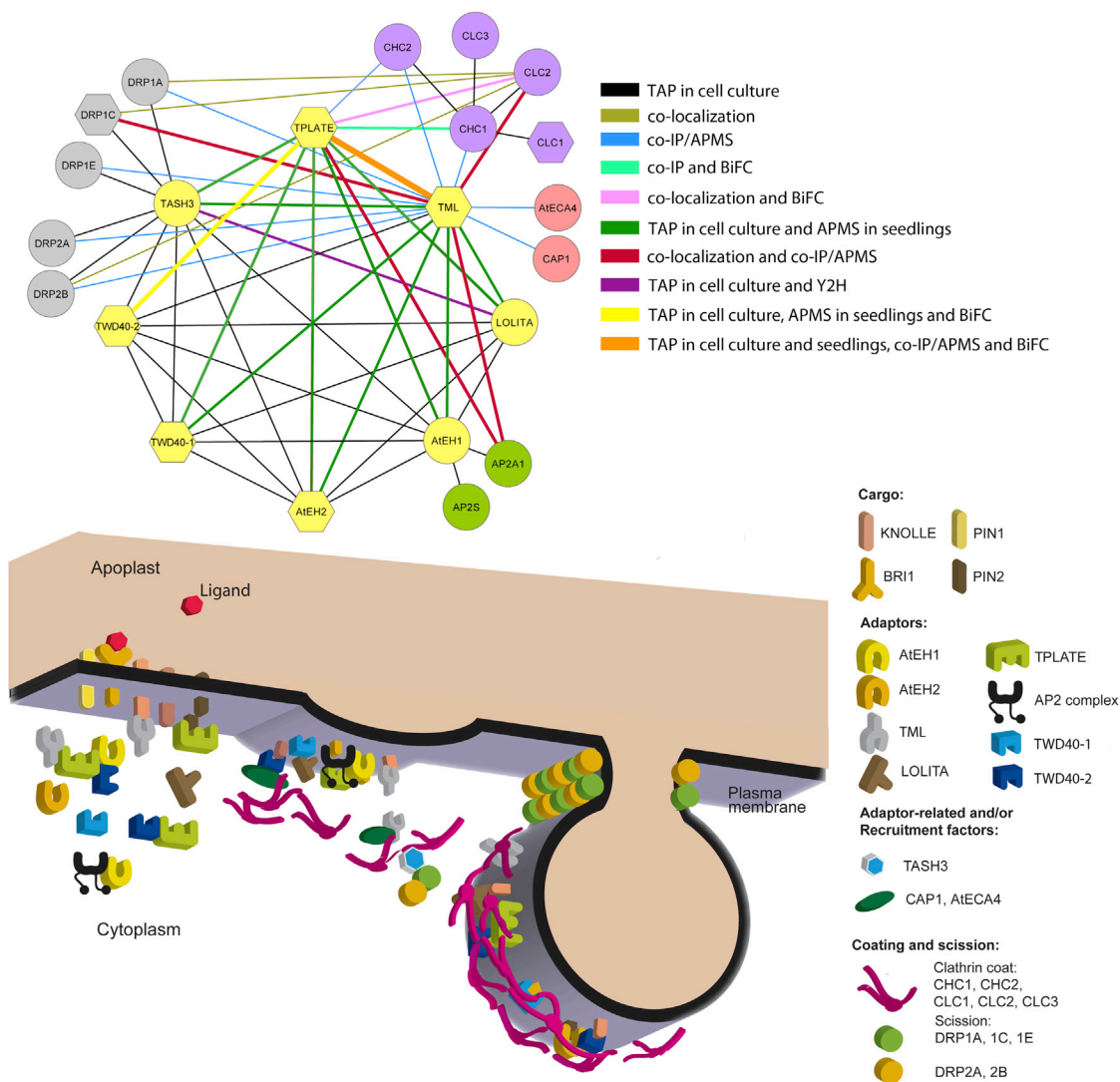


Figure 6. Overview of Interactions and Model of Clathrin-Mediated Endocytosis in Plants

Cytoscape model (top) summarizing all known interactions between the various subunits from this work and previous reports. Edge colors represent the experiments listed. Node colors represent the different protein families and subcomplexes. Yellow, TPC; gray, DRPs; purple, clathrin proteins; green, *Arabidopsis* AP2 subunits; and pink, ANTH domain-containing proteins. The polygonal node shape of some subunits refers to their male sterile phenotype when mutated as shown in this manuscript and previous reports. The model (bottom) provides a visual representation of the findings outlined in this manuscript.

they are certainly not required for it. As the colocalization experiments were performed on genetic knockout mutants of TPLATE and TML, dynamic TPC-negative but AP2-positive foci cannot be the result of competition between the endogenous and fluorescent forms of these proteins. While it is unclear if all foci corre-

spond to recognition and internalization of specific cargo, or perhaps also to nonfunctional adaptor recruitment at the PM, it is clear that loss of TPC function is detrimental to CME and plant development. The latter is likely caused by strong effects on endocytosis leading to severe misregulation of signaling and

(E and F) Representative immunolocalizations and quantification of fluorescence intensity in BFA bodies of endogenous PIN1 and PIN2 proteins after BFA treatment (50 μ M; 30 min) in control seedlings (Φ estradiol) or seedlings expressing *amiR-TML* grown on beta-estradiol (ami estradiol). Induction of *amiR-TML* reduces PIN1 and PIN2 accumulation in BFA bodies (Student's t test; p value < 0.0001, triple asterisk; n = 112, 4 roots and n = 60, 6 roots for PIN1 and PIN2 for control cells and n = 207, 14 roots and n = 83, 9 roots for PIN1 and PIN2 for *amiR-TML* cells).

(G and H) Representative immunolocalizations and quantification of cells with PM labeling of endogenous KNOLLE protein in control seedlings (Φ estradiol; n = 86, 17 roots) and seedlings expressing *amiR-TML* (ami estradiol; n = 175, 25 roots). Induction of *amiR-TML* results in ectopic accumulation of KNOLLE at the cortical division zone or the PM (arrowheads) in contrast to the control (Φ estradiol).

Error bars represent SEM. Scale bars, 10 μ m. See also Figure S5.

transport processes at the PM thereby affecting cell viability. On the other hand, loss of AP2 function in plants only results in very mild phenotypic outcomes (Fan et al., 2013; Kim et al., 2013; Yamaoka et al., 2013). These observations suggest that the TPC represents the main endocytic adaptor-related complex of plants.

The TPC Is Required for the Internalization of a Multitude of Endocytic Cargo Molecules

If the TPC acts as the major adaptor complex for CME in plants, serious defects in internalization of endocytic markers in TPC compromised cells can be anticipated. Constitutive and inducible silencing of *TPLATE* and *TML* strongly inhibited the uptake of the endocytic tracer FM4-64 and the recently reported BRI1 ligand AFCS (Irani et al., 2012). The latter is reminiscent of the blocked AFCS uptake in clathrin-impaired *Arabidopsis* root cells which also leads to pronounced accumulation of AFCS at the cell surface (Irani et al., 2012). Given the strong plant phenotypes resulting from the expression of HUB1 (Kitakura et al., 2011), DN-ARA7 (Dhonukshe et al., 2008), and *amiR-TML*, a general defect in endocytosis could result in altered cell wall composition and therefore a changed affinity of AFCS to this compartment. The AFCS uptake corroborates the link between the TPC and clathrin and is in agreement with the drastic inhibition of ligand uptake upon FCHO downregulation in animal cells (Henne et al., 2010). Furthermore, the trafficking of several PM proteins associated with signaling, polarity and transport was altered in TPC deficient cells. This shows that the TPC is associated with the internalization of many different types of cargo molecules.

Our findings show that plants have evolved a distinct adaptor complex consisting of eight core proteins that regulates CME. The overall protein sequences of the subunits have diverged to the extent that no reliable homology can be inferred beyond the presence of specific domains. Yet, these proteins may have retained unrecognized structural homology to animal and yeast counterparts. This works as an intriguing example for how a conserved process, such as CME, holds proteins with drastic changes in protein sequences that fulfill related biological functions. We therefore propose that the discovery of the TPC, together with knowledge about the CME machineries in yeast and animals, may form a solid platform to explore evolutionary questions related to adaptor-cargo recognition and discrimination.

EXPERIMENTAL PROCEDURES

A detailed overview of all experimental procedures can be found in the [Extended Experimental Procedures](#).

Protein Complex Isolation

Tandem affinity purification (TAP-tag) experiments were performed on *Arabidopsis* cell culture cells (PSB-D) with protein G and Streptavidin-binding peptide (GS)-tagged bait proteins according to (Van Leene et al., 2011).

APMS and coIP experiments for *TPLATE*-GFP, *TML*-GFP, and *TML*-YFP were performed using a GFP-trap system (Chromotek and Miltenyi Biotec) on *Arabidopsis* seedlings expressing functional fusion proteins in the respective complemented mutant (*tplate*, *tml-1*, and *tml-2*) backgrounds. APMS experiments on GFP-TML, GFP-TMLΔC, and Venus-TMLΔC were performed on *Arabidopsis* seedlings in the wild-type (Col-0) background or on PSB-D cells.

Phylogenetic Analysis

Protein sequences were aligned using MSAProbs v0.97 (Liu et al., 2010) and cleaned up as described in (Vandepoele et al., 2004). ProtTest v2.4 (Abascal et al., 2005) was used to score different models of protein evolution and identified the LG+I+G+F model as best fit, with a substantial lead over other models. MrBayes v3.1.2 (Huelsenbeck and Ronquist, 2001) was used for constructing the phylogeny. The BMCMC was run for 10⁶ generations, with two parallel runs of four chains each, sampling every 100 generations and discarding the first 2,500 samples as burn-in. Proper MCMC convergence was checked using the AWTY web program (Nylander et al., 2008) and the remaining 7,501 samples were used to construct the 50% majority-rule consensus phylogeny.

VAEM and Spinning Disc Microscopy

Variable angle epifluorescence (VAEM) and spinning disc microscopy were conducted on a Nikon Ti microscope equipped with either a manual VAEM arm or a CSU-X1 spinning disc head (Yokogawa, Tokyo, Japan) equipped with a CFI Apo TIRF 100× NA1.49 oil immersion objective and an Evolve EMCCD camera (Photometrics Technology, Tucson AZ, USA).

Quantification of Fluorescence Intensities

Quantifications of fluorescence intensities were done on nonsaturated images by normalizing the maximal fluorescence intensity present in BFA bodies or cell plates to the respective PM or cytoplasmic intensity by indicating them as a ROI using the Olympus FluoViewer10-ASW 2.1 or the imageJ (Rasband, W.S. National Institute of Health) software packages.

SUPPLEMENTAL INFORMATION

Supplemental Information includes Extended Experimental Procedures, five figures, five movies, and four tables and can be found with this article online at <http://dx.doi.org/10.1016/j.cell.2014.01.039>.

AUTHOR CONTRIBUTIONS

A.G., C.S.R., S.V., S.D.R., H.Z., K.V., D.E., J.R.M., M.A., U.K., K.G., E.W. and D.V.D. designed, performed and analyzed experiments. J.V.L., A.S., T.K., S.M., S.Y.B., J.F., E.R., S.P. and G.D.J. designed and analyzed experiments. N.D.W., G.P., E.V.D.S., B.C., L.V. and M.E. performed experiments. A.G., C.S.R., S.V., S.P., G.D.J. and D.V.D. wrote the paper. All authors read and contributed to the finalization of the paper. A.G. and C.S.R. share equal first authorship and S.P., G.D.J. and D.V.D. share equal senior authorship.

ACKNOWLEDGMENTS

The authors would like to thank Wim Grunewald (VIB/UGent, Belgium), Niko Geldner (University of Lausanne, Switzerland), Satoshi Naramoto and Masaru Fujimoto (University of Tokyo, Japan), Inhwan Hwang (Pohang University, Korea), Gerd Jürgens (Tübingen University, Germany), and Christian Luschnig (Vienna University, Austria) for sharing materials; Mansour Karimi and Riet De Rycke (VIB/University of Ghent, Belgium) for vector cloning and IEM attempts; and Luis Vidali (Worcester Polytechnic Institute, USA) for constructive discussions. A.G. was indebted to the Agency for Innovation by Science and Technology for a predoctoral fellowship. S.P. and C.S.R. were funded through the Max-Planck Gesellschaft. K.V., S.V., J.V.L. and S.M. are fellows of the Research Foundation - Flanders (FWO). S.D.R. was funded by the Marie-Curie Initial Training Network BRAVISSIMO (PITN-GA-2008-215118). J.R.M. and S.Y.B. were supported by the National Science Foundation (1121998) (S.Y.B.). Part of this work was carried out using the Stevin Supercomputer Infrastructure at Ghent University, funded by Ghent University, the Hercules Foundation, and the Flemish Government-department EWI. We apologize to colleagues whose work could not be cited due to space limitations.

Received: June 7, 2013

Revised: October 28, 2013

Accepted: January 16, 2014

Published: February 13, 2014

REFERENCES

- Abascal, F., Zardoya, R., and Posada, D. (2005). ProtTest: selection of best-fit models of protein evolution. *Bioinformatics* 21, 2104–2105.
- Backues, S.K., Korasick, D.A., Heese, A., and Bednarek, S.Y. (2010). The Arabidopsis dynamin-related protein2 family is essential for gametophyte development. *Plant Cell* 22, 3218–3231.
- Bar, M., Aharon, M., Benjamin, S., Rotblat, B., Horowitz, M., and Avni, A. (2008). AtEHDs, novel Arabidopsis EH-domain-containing proteins involved in endocytosis. *Plant J.* 55, 1025–1038.
- Bar, M., Sharfman, M., Schuster, S., and Avni, A. (2009). The coiled-coil domain of EHD2 mediates inhibition of LeEix2 endocytosis and signaling. *PLoS ONE* 4, e7973.
- Barberon, M., Zelazny, E., Robert, S., Conéjéro, G., Curie, C., Friml, J., and Vert, G. (2011). Monoubiquitin-dependent endocytosis of the iron-regulated transporter 1 (IRT1) transporter controls iron uptake in plants. *Proc. Natl. Acad. Sci. USA* 108, E450–E458.
- Barth, M., and Holstein, S.E. (2004). Identification and functional characterization of Arabidopsis AP180, a binding partner of plant alphaC-adaptin. *J. Cell Sci.* 117, 2051–2062.
- Boettner, D.R., Chi, R.J., and Lemmon, S.K. (2012). Lessons from yeast for clathrin-mediated endocytosis. *Nat. Cell Biol.* 14, 2–10.
- Boutté, Y., Frescatada-Rosa, M., Men, S., Chow, C.M., Ebine, K., Gustavsson, A., Johansson, L., Ueda, T., Moore, I., Jürgens, G., and Grebe, M. (2010). Endocytosis restricts Arabidopsis KNOLLE syntaxin to the cell division plane during late cytokinesis. *EMBO J.* 29, 546–558.
- Chen, X., Irani, N.G., and Friml, J. (2011). Clathrin-mediated endocytosis: the gateway into plant cells. *Curr. Opin. Plant Biol.* 14, 674–682.
- Cocucci, E., Aguet, F., Boulant, S., and Kirchhausen, T. (2012). The first five seconds in the life of a clathrin-coated pit. *Cell* 150, 495–507.
- Collings, D.A., Gebbie, L.K., Howles, P.A., Hurley, U.A., Birch, R.J., Cork, A.H., Hocart, C.H., Arioli, T., and Williamson, R.E. (2008). Arabidopsis dynamin-like protein DRP1A: a null mutant with widespread defects in endocytosis, cellulose synthesis, cytokinesis, and cell expansion. *J. Exp. Bot.* 59, 361–376.
- Collins, B.M., McCoy, A.J., Kent, H.M., Evans, P.R., and Owen, D.J. (2002). Molecular architecture and functional model of the endocytic AP2 complex. *Cell* 109, 523–535.
- Conibear, E. (2010). Converging views of endocytosis in yeast and mammals. *Curr. Opin. Cell Biol.* 22, 513–518.
- Curtis, M.D., and Grossniklaus, U. (2003). A gateway cloning vector set for high-throughput functional analysis of genes in planta. *Plant Physiol.* 133, 462–469.
- Detmer, J., Hong-Hermesdorf, A., Stierhof, Y.D., and Schumacher, K. (2006). Vacuolar H⁺-ATPase activity is required for endocytic and secretory trafficking in Arabidopsis. *Plant Cell* 18, 715–730.
- Dhonukshe, P., Aliento, F., Hwang, I., Robinson, D.G., Mravec, J., Stierhof, Y.D., and Friml, J. (2007). Clathrin-mediated constitutive endocytosis of PIN auxin efflux carriers in Arabidopsis. *Curr. Biol.* 17, 520–527.
- Dhonukshe, P., Tanaka, H., Goh, T., Ebine, K., Mähönen, A.P., Prasad, K., Bliou, I., Geldner, N., Xu, J., Uemura, T., et al. (2008). Generation of cell polarity in plants links endocytosis, auxin distribution and cell fate decisions. *Nature* 456, 962–966.
- Di Rubbo, S., Irani, N.G., Kim, S.Y., Xu, Z.Y., Gadeyne, A., Dejonghe, W., Vanhoutte, I., Persiau, G., Eeckhout, D., Simon, S., et al. (2013). The clathrin adaptor complex AP-2 mediates endocytosis of brassinosteroid insensitive1 in Arabidopsis. *Plant Cell* 25, 2986–2997.
- Du, Y., Tejos, R., Beck, M., Himschoot, E., Li, H., Robatzek, S., Vanneste, S., and Friml, J. (2013). Salicylic acid interferes with clathrin-mediated endocytic protein trafficking. *Proc. Natl. Acad. Sci. USA* 110, 7946–7951.
- Fan, L., Hao, H., Xue, Y., Zhang, L., Song, K., Ding, Z., Botella, M.A., Wang, H., and Lin, J. (2013). Dynamic analysis of Arabidopsis AP2 σ subunit reveals a key role in clathrin-mediated endocytosis and plant development. *Development* 140, 3826–3837.
- Fujimoto, M., Arimura, S., Ueda, T., Takanashi, H., Hayashi, Y., Nakano, A., and Tsutsumi, N. (2010). Arabidopsis dynamin-related proteins DRP2B and DRP1A participate together in clathrin-coated vesicle formation during endocytosis. *Proc. Natl. Acad. Sci. USA* 107, 6094–6099.
- Geldner, N., Friml, J., Stierhof, Y.D., Jürgens, G., and Palme, K. (2001). Auxin transport inhibitors block PIN1 cycling and vesicle trafficking. *Nature* 413, 425–428.
- Geldner, N., Anders, N., Wolters, H., Keicher, J., Kornberger, W., Müller, P., Delbarre, A., Ueda, T., Nakano, A., and Jürgens, G. (2003). The Arabidopsis GNOM ARF-GEF mediates endosomal recycling, auxin transport, and auxin-dependent plant growth. *Cell* 112, 219–230.
- Geldner, N., Hyman, D.L., Wang, X., Schumacher, K., and Chory, J. (2007). Endosomal signaling of plant steroid receptor kinase BRI1. *Genes Dev.* 21, 1598–1602.
- Grebe, M., Xu, J., Möbius, W., Ueda, T., Nakano, A., Geuze, H.J., Rook, M.B., and Scheres, B. (2003). Arabidopsis sterol endocytosis involves actin-mediated trafficking via ARA6-positive early endosomes. *Curr. Biol.* 13, 1378–1387.
- Henne, W.M., Boucrot, E., Meinecke, M., Evergren, E., Vallis, Y., Mittal, R., and McMahon, H.T. (2010). FCHO proteins are nucleators of clathrin-mediated endocytosis. *Science* 328, 1281–1284.
- Huelsenbeck, J.P., and Ronquist, F. (2001). MRBAYES: Bayesian inference of phylogenetic trees. *Bioinformatics* 17, 754–755.
- Irani, N.G., Di Rubbo, S., Mylle, E., Van den Begin, J., Schneider-Pizoñ, J., Hnilíková, J., Šiša, M., Buyst, D., Vilarasa-Blasi, J., Szatmári, A.M., et al. (2012). Fluorescent castasterone reveals BRI1 signaling from the plasma membrane. *Nat. Chem. Biol.* 8, 583–589.
- Kang, B.H., Busse, J.S., and Bednarek, S.Y. (2003). Members of the Arabidopsis dynamin-like gene family, ADL1, are essential for plant cytokinesis and polarized cell growth. *Plant Cell* 15, 899–913.
- Kim, S.Y., Xu, Z.Y., Song, K., Kim, D.H., Kang, H., Reichardt, I., Sohn, E.J., Friml, J., Juergens, G., and Hwang, I. (2013). Adaptor protein complex 2-mediated endocytosis is crucial for male reproductive organ development in Arabidopsis. *Plant Cell* 25, 2970–2985.
- Kitakura, S., Vanneste, S., Robert, S., Löffke, C., Teichmann, T., Tanaka, H., and Friml, J. (2011). Clathrin mediates endocytosis and polar distribution of PIN auxin transporters in Arabidopsis. *Plant Cell* 23, 1920–1931.
- Konopka, C.A., Backues, S.K., and Bednarek, S.Y. (2008). Dynamics of Arabidopsis dynamin-related protein 1C and a clathrin light chain at the plasma membrane. *Plant Cell* 20, 1363–1380.
- Kukulski, W., Schorb, M., Kaksonen, M., and Briggs, J.A. (2012). Plasma membrane reshaping during endocytosis is revealed by time-resolved electron tomography. *Cell* 150, 508–520.
- Lam, B.C., Sage, T.L., Bianchi, F., and Blumwald, E. (2001). Role of SH3 domain-containing proteins in clathrin-mediated vesicle trafficking in Arabidopsis. *Plant Cell* 13, 2499–2512.
- Liu, Y., Schmidt, B., and Maskell, D.L. (2010). MSAProbs: multiple sequence alignment based on pair hidden Markov models and partition function posterior probabilities. *Bioinformatics* 26, 1958–1964.
- Macia, E., Ehrlich, M., Massol, R., Boucrot, E., Brunner, C., and Kirchhausen, T. (2006). Dynasore, a cell-permeable inhibitor of dynamin. *Dev. Cell* 10, 839–850.
- Marhavý, P., Bielach, A., Abas, L., Abuzeineh, A., Duclercq, J., Tanaka, H., Páezová, M., Petrásek, J., Friml, J., Kleine-Vehn, J., and Benková, E. (2011). Cytokinin modulates endocytic trafficking of PIN1 auxin efflux carrier to control plant organogenesis. *Dev. Cell* 21, 796–804.
- Mayers, J.R., Wang, L., Pramanik, J., Johnson, A., Sarkeshik, A., Wang, Y., Saengsawang, W., Yates, J.R., 3rd, and Audhya, A. (2013). Regulation of ubiquitin-dependent cargo sorting by multiple endocytic adaptors at the plasma membrane. *Proc. Natl. Acad. Sci. USA* 110, 11857–11862.
- McMahon, H.T., and Boucrot, E. (2011). Molecular mechanism and physiological functions of clathrin-mediated endocytosis. *Nat. Rev. Mol. Cell Biol.* 12, 517–533.

- Mooren, O.L., Galletta, B.J., and Cooper, J.A. (2012). Roles for actin assembly in endocytosis. *Annu. Rev. Biochem.* **81**, 661–686.
- Nagawa, S., Xu, T., Lin, D., Dhonukshe, P., Zhang, X., Friml, J., Scheres, B., Fu, Y., and Yang, Z. (2012). ROP GTPase-dependent actin microfilaments promote PIN1 polarization by localized inhibition of clathrin-dependent endocytosis. *PLoS Biol.* **10**, e1001299.
- Nylander, J.A., Wilgenbusch, J.C., Warren, D.L., and Swofford, D.L. (2008). AWTY (are we there yet?): a system for graphical exploration of MCMC convergence in Bayesian phylogenetics. *Bioinformatics* **24**, 581–583.
- Petrásek, J., Mravec, J., Bouchard, R., Blakeslee, J.J., Abas, M., Seifertová, D., Wisniewska, J., Tadele, Z., Kubes, M., Covanová, M., et al. (2006). PIN proteins perform a rate-limiting function in cellular auxin efflux. *Science* **312**, 914–918.
- Reider, A., Barker, S.L., Mishra, S.K., Im, Y.J., Maldonado-Báez, L., Hurley, J.H., Traub, L.M., and Wendland, B. (2009). Syp1 is a conserved endocytic adaptor that contains domains involved in cargo selection and membrane tubulation. *EMBO J.* **28**, 3103–3116.
- Robatzek, S., Chinchilla, D., and Boller, T. (2006). Ligand-induced endocytosis of the pattern recognition receptor FLS2 in Arabidopsis. *Genes Dev.* **20**, 537–542.
- Robert, S., Kleine-Vehn, J., Barbez, E., Sauer, M., Paciorek, T., Baster, P., Vanneste, S., Zhang, J., Simon, S., Covanová, M., et al. (2010). ABP1 mediates auxin inhibition of clathrin-dependent endocytosis in Arabidopsis. *Cell* **143**, 111–121.
- Schwab, R., Ossowski, S., Riester, M., Warthmann, N., and Weigel, D. (2006). Highly specific gene silencing by artificial microRNAs in Arabidopsis. *Plant Cell* **18**, 1121–1133.
- Smaczynska-de Rooij, I.I., Allwood, E.G., Aghamohammadzadeh, S., Hettema, E.H., Goldberg, M.W., and Ayscough, K.R. (2010). A role for the dynamin-like protein Vps1 during endocytosis in yeast. *J. Cell Sci.* **123**, 3496–3506.
- Song, K., Jang, M., Kim, S.Y., Lee, G., Lee, G.J., Kim, D.H., Lee, Y., Cho, W., and Hwang, I. (2012). An A/ENTH domain-containing protein functions as an adaptor for clathrin-coated vesicles on the growing cell plate in Arabidopsis root cells. *Plant Physiol.* **159**, 1013–1025.
- Sutter, J.U., Sieben, C., Hartel, A., Eisenach, C., Thiel, G., and Blatt, M.R. (2007). Abscisic acid triggers the endocytosis of the Arabidopsis KAT1 K⁺ channel and its recycling to the plasma membrane. *Curr. Biol.* **17**, 1396–1402.
- Takano, J., Tanaka, M., Toyoda, A., Miwa, K., Kasai, K., Fujii, K., Onouchi, H., Naito, S., and Fujiwara, T. (2010). Polar localization and degradation of Arabidopsis boron transporters through distinct trafficking pathways. *Proc. Natl. Acad. Sci. USA* **107**, 5220–5225.
- Tanaka, H., Kitakura, S., De Rycke, R., De Groot, R., and Friml, J. (2009). Fluorescence imaging-based screen identifies ARF GEF component of early endosomal trafficking. *Curr. Biol.* **19**, 391–397.
- Tebar, F., Sorkina, T., Sorkin, A., Ericsson, M., and Kirchhausen, T. (1996). Eps15 is a component of clathrin-coated pits and vesicles and is located at the rim of coated pits. *J. Biol. Chem.* **271**, 28727–28730.
- Umasankar, P.K., Sanker, S., Thieman, J.R., Chakraborty, S., Wendland, B., Tsang, M., and Traub, L.M. (2012). Distinct and separable activities of the endocytic clathrin-coat components Fcho1/2 and AP-2 in developmental patterning. *Nat. Cell Biol.* **14**, 488–501.
- Van Damme, D., Coutuer, S., De Rycke, R., Bouget, F.Y., Inzé, D., and Geelen, D. (2006). Somatic cytokinesis and pollen maturation in Arabidopsis depend on TPLATE, which has domains similar to coat proteins. *Plant Cell* **18**, 3502–3518.
- Van Damme, D., Gadeyne, A., Vanstraelen, M., Inzé, D., Van Montagu, M.C., De Jaeger, G., Russinova, E., and Geelen, D. (2011). Adaptin-like protein TPLATE and clathrin recruitment during plant somatic cytokinesis occurs via two distinct pathways. *Proc. Natl. Acad. Sci. USA* **108**, 615–620.
- Van Leene, J., Eeckhout, D., Persiau, G., Van De Slijke, E., Geerinck, J., Van Isterdael, G., Witters, E., and De Jaeger, G. (2011). Isolation of transcription factor complexes from Arabidopsis cell suspension cultures by tandem affinity purification. *Methods Mol. Biol.* **754**, 195–218.
- Vandepoele, K., De Vos, W., Taylor, J.S., Meyer, A., and Van de Peer, Y. (2004). Major events in the genome evolution of vertebrates: paranome age and size differ considerably between ray-finned fishes and land vertebrates. *Proc. Natl. Acad. Sci. USA* **101**, 1638–1643.
- Wang, C., Yan, X., Chen, Q., Jiang, N., Fu, W., Ma, B., Liu, J., Li, C., Bednarek, S.Y., and Pan, J. (2013). Clathrin light chains regulate clathrin-mediated trafficking, auxin signaling, and development in Arabidopsis. *Plant Cell* **25**, 499–516.
- Yamaoka, S., Shimono, Y., Shirakawa, M., Fukao, Y., Kawase, T., Hatsugai, N., Tamura, K., Shimada, T., and Hara-Nishimura, I. (2013). Identification and dynamics of Arabidopsis adaptor protein-2 complex and its involvement in floral organ development. *Plant Cell* **25**, 2958–2969.
- Yeung, B.G., Phan, H.L., and Payne, G.S. (1999). Adaptor complex-independent clathrin function in yeast. *Mol. Biol. Cell* **10**, 3643–3659.